One-dimensional Phosphorus Nanostructures: from Nanorings to Nanohelices

One–dimensional Phosphorus Nanostructures: from Nanorings to Nanohelices.

Giuseppe Sansone,[1] Lorenzo Maschio,[2] and Antti J. Karttunen[3]

[1]*Dipartimento di Chimica, Università di Torino, Via P. Giuria 5, 10125 Torino, Italy*
[2]*Dipartimento di Chimica, C3S centre, NIS centre, Università di Torino, Via P. Giuria 5, 10125 Torino, Italy*
[3]*Department of Chemistry and Materials Science, Aalto University, Kemistintie 1, 02150 Espoo, Finland**

(Dated: September 19, 2017)

Abstract: Phosphorus nanorings and nanohelices – which were speculated to exist over 20 years ago – have been systematically derived from one parent structure and studied with quantum chemical methods. The $(P_8P_2)_n$ nanorings have been recently synthetized inside carbon nanotube templates, and our comprehensive analysis of possible structural arrangements strongly supports the possibility to experimentally realize the closely-related $(P_8P_2)_n$ nanohelices. The nanohelices possess very low stiffness, suggesting interesting mechanical properties with nano–spring -like behavior.

Phosphorus shows very rich allotropy, making it an exciting element from the point of view of fundamental structural chemistry as well as new materials.[1,2] The allotropes of phosphorus are divided in three main classes: white, black, and red phosphorus. White phosphorus is simply composed of P_4 molecules. Black phosphorus is a layered material composed of rather weakly bound 2D sheets, which can be exfoliated to create phosphorene, a 2D allotrope of significant interest.[3,4] Red phosphorus is the most diverse class of phosphorus allotropes, including several crystalline modifications together with various amorphous polymeric networks. The current understanding and energetics of the various red-P allotropes have been discussed comprehensively by Weihrich et al.[1,5] Among the red phosphorus modifications, X-ray crystal structures have been obtained for fibrous red and violet phosphorus.[6–8] In addition, two types of structurally characterized nanorods have been extracted from their copper iodide adducts.[9] Using a simplified notation, the nanorods are one-dimensional P_{12} chains composed of $-P_4-P_8-$ or $-P_2-P_{10}-$ building blocks.

The building blocks of red phosphorus have been studied computationally since early 1990s.[10–12] In 1995, Böcker and Häser presented a comprehensive theoretical study on the building blocks of red phosphorus and they were able to predict the existence of several red phosphorus modifications.[13] Böcker and Häser also studied red phosphorus chains composed of $-P_2-P_8-$ building blocks and found out that such chains bend spontaneously, leading to hypothesis that $-P_2-P_8-$ building block would result in the formation of $(P_8P_2)_n$ rings and macrohelices.[28] The ring-shaped $(P_8P_2)_n$ allotropes were later studied in detail theoretically and the rings were predicted to show a energy minimum at around 160–200 atoms.[14,15] Notably, recent investigation of phosphorus nanostructures inside carbon nanotubes (CNT) suggested the nanostructures to be stacked $(P_8P_2)_n$ rings and high-resolution transmission electron microscopy (HR-TEM) images were compared with a model of stacked P230 rings.[16],[29] In addition to the $(P_8P_2)_n$ rings, a route towards the helical structures postulated by Böcker and Häser has been suggested recently by Tománek *et al.*,[17] who applied an analytical model to investigate the energetics of the hypothetical $(P_8P_2)_n$ helices (coils). We note that a very different type of phosphorus helix has been recently observed as a part of an inorganic double helix in semiconducting SnIP.[18]

Here we investigate $(P_8P_2)_n$ nanorings and nanohelices with quantum chemical methods and show how both the rings and helices can be derived systematically from one parent structure. By using a novel computational scheme implemented in the CRYSTAL program package,[19] we are able to carry out full structural optimizations on phosphorus nanohelices as large as 5770 atoms in the unit cell. Our calculations reveal the full structural details of phosphorus nanohelices with varying "chirality", allowing us to analyze the energetics and feasibility of the $(P_8P_2)_n$ nanorings and nanohelices.

The helices and stacked rings studied here are one-dimensional (1D) periodic structures. Similar to carbon nanotubes, helices and stacked rings can be derived by rolling up a suitable 2D slab. Figure 1 illustrates the building principles of the $(P_8P_2)_n$ nanorings and nanohelices. The starting point is the $-P_2-P_8-$ building block (Figure 1a) that is known to form curved structural units.[13,14,17] The $-P_2-P_8-$ building block is then used to form a 1D $P_8P_2)_n$ chain (Figure 1b) and a 2D slab composed of parallel $(P_8P_2)_n$ chains (Figure 1c). The final key step is then to coil the slab according to so-called rolling vector $\mathbf{R}$, Figure 1c.

The rolling vector is defined as $\mathbf{R} = n_1\mathbf{a}_1+n_2\mathbf{a}_2$, where $\{\mathbf{a}_i\}$ are the slab unit cell vectors and $\{n_i\}$ define the so-called chirality of the helix. The concept of chirality is analogous to the chirality of CNTs rolled up from a hexagonal graphene sheet.[20] The phosphorus helices and rings can be described conveniently using notation (n_1, n_2). As shown in Figure 1c for the $(8,n_2)$ series, the primitive cell of the slab is square-shaped. The so-called chiral angle, θ, is shown for different rolling vectors.[30]

In contrast to CNTs rolled up from a graphene sheet with only covalent bonds, the $(P_8P_2)_n$ helices and rings possess weak non-covalent interactions between individual $(P_8P_2)_n$ chains. Proper theoretical treatment of these weak interactions is crucial for understanding the

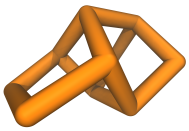

(a) $-P_2-P_8-$ building block.

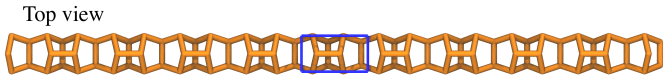

(b) $(P_8P_2)_n$ chain generated by periodic repetition of the $-P_2-P_8-$ building block along the (n_1,0) direction (blue rectangle shows the unit cell).

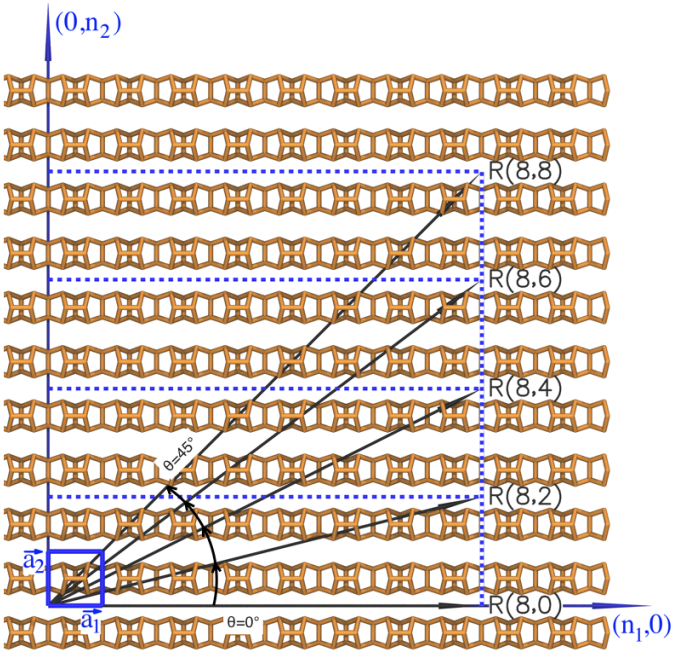

(c) Rolling procedure of a 2D slab which has been generated by periodic repetition of $(P_8P_2)_n$ chains along the (0,n_2) direction (blue square shows the unit cell).

Figure 1: A schematic summary of the building principles of the $(P_8P_2)_n$ nanorings and nanohelices.

energetics of the nanostructures. Another fundamental difference in comparison to CNTs is the the role of n_2: in a CNT, n_2 simply determines the chirality of the tube, but for the phosphorus helices, values of $n_2 > 1$ additionally set the number of chains to be rolled up simultaneously (*vide infra*). We will discuss separately the cases $n_2 = 0$, $n_2 = 1$ and $n_2 > 1$, in this order.

We start our structural discussion from the special case of $n_2 = 0$, that is, structures $(n_1, 0)$. This family is built up by coiling a single chain of a given length along the (n_1,0) direction and stacking the so-obtained rings. An example is shown as the topmost structure in Figure 2. The individual rings in the stack correspond to the previously studied phosphorus nanorings.[14] For example, the rings in the (20,0) stack correspond to P_{200} rings studied previously.

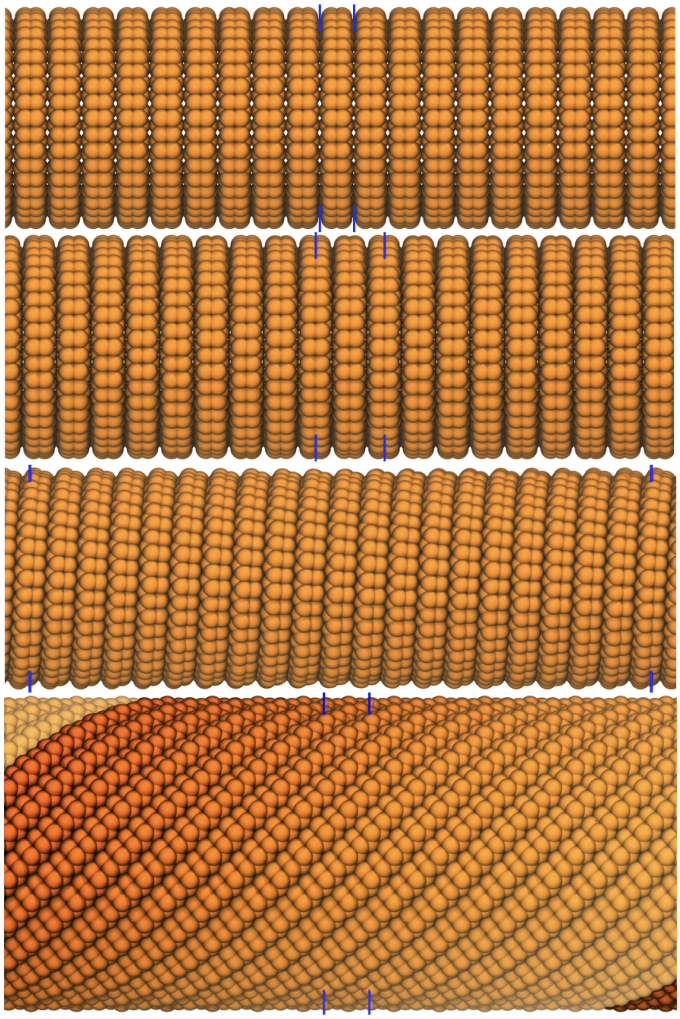

Figure 2: Side views of various $(P_8P_2)_n$ nanostructures with different (n_1,n_2) chiralities (space-filling representation for clarity). From top to bottom: 1) (20,0) = eclipsed stacked P_{200} rings, 2) (20,0) = staggered stacked P_{200} rings, 3) (20,1) = single-chain helix, and 4) (20,20) = multi-chain helix. Blue lines denote the primitive cell for each structure. The (20,20) structure has 20 intertwined helices, which are illustrated with a color gradient from dark to light.

The unit cell shown in Figure 1c only allows to model structures, where the stacked rings are "eclipsed", because all the phosphorus chains are perfectly aligned in parallel. Thus, we also studied (n_1,0) structures built by using a double unit cell, where two phosphorus chains are displaced with respect to each other analogously to the AB stacking of chains discussed by Tománek *et al.* (see Supporting information for full discussion on the stacking).[17] An example of the resulting "staggered" stacked rings is shown as the second structure from the top in Figure 2. The staggered rings adopt kind of a key-lock configuration, where the attractive inter-ring disper-

sion interactions are maximized.

Figure 3 illustrates the relative energies of the stacked $(P_8P_2)_n$ rings, that is, $(n_1,0)$ structures (relative energies plotted in all figures are tabulated in the Supporting Information). The level of theory is DFT-PBE0-D3/TZVPP, which includes dispersion corrections for the inter-ring van der Waals interactions. We found a similar stability trend for both staggered and eclipsed rings. The (8,0) rings are, small, strained, and less stable than a straight $(P_8P_2)_n$ chain. However, starting from (12,0), both eclipsed and staggered stacked rings are clearly more stable than the straight chain. The rings reach an energy minimum at (20,0), that is, stacked P_{200} rings, after which the relative energy slowly starts to increase. This finding is in agreement with previous study, whre the isolated P_{200} ring was predicted to be the minimum energy structure among P_{80}-P_{360} rings.[14]

The staggered stacked rings are about 1 kJ/mol per atom more stable than the eclipsed structures. We also carried out harmonic frequency calculations on the stacked $(P_8P_2)_n$ rings to find out if they are true local minima. Analogously to previous work,[14] we found that isolated rings starting from P_{120} are true local minima. In the case of stacked $(P_8P_2)_n$ rings showing inter-ring van der Waals dispersion interactions, we found that the staggered (12,0) structure is also a true local minimum. However, the eclipsed stacked rings up to (20,0) have imaginary vibrational modes corresponding to twisting motion where the atoms vibrate along the stacking direction of the rings. In comparison to known phosphorus allotropes, the staggered stacked P_{200} rings are 11.1 kJ/mol per atom more stable than white phosphorus, P_4, but 8.1 and 8.2 kJ/mol per atom less stable than fibrous red and black phosphorus, respectively.

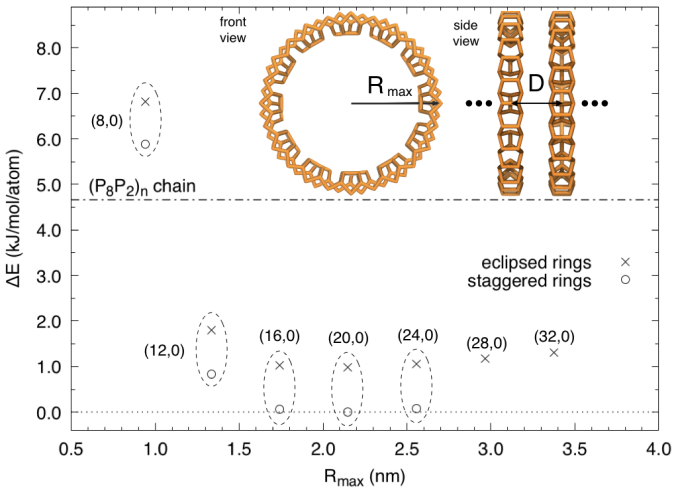

Figure 3: The relative energy of the eclipsed and staggered stacked $(P_8P_2)_n$ rings, $(n_1,0)$, as a function of the maximum ring radius R_{max}. The top inset shows the definition of R_{max} and the inter-ring distance D for stacked (12,0) rings (P_{120}).

In the case of the phosphorus nanostructures recently synthetized inside CNTs,[16] Zhang *et al.* superimposed a structure model of stacked P230 rings on their experimental HRTEM images. In their model, the diameter and the inter-ring distance (D) were 5.30 nm and 0.64 nm respectively. For comparison, the staggered (24,0) structure studied here contains P_{240} rings with diameter and D of 5.47 nm and 0.68 nm, respectively[31]. In the case of the eclipsed (24,0) structure, D is 0.73 nm.

After the stacked ring structures with rolling vectors of $(n_1,0)$, we move to structures where n_2 has non-zero values. We first discuss the $(n_1,1)$ structures, which correspond to coiling a single $(P_8P_2)_n$ chain into a helix. The inset in the top of Figure 4 illustrates a (20,1) helix and the third subfigure in Figure 2 shows the same helix using a space-filling representation. The latter view is not very different from the staggered stacked P_{200} rings shown as the second subfigure in Figure 2. However, the unit cells are very different: The (20,1) helix has 4010 atoms in the unit cell, while the (20,0) structure has only 400 or 200 atoms for the staggered and eclipsed cases, respectively.

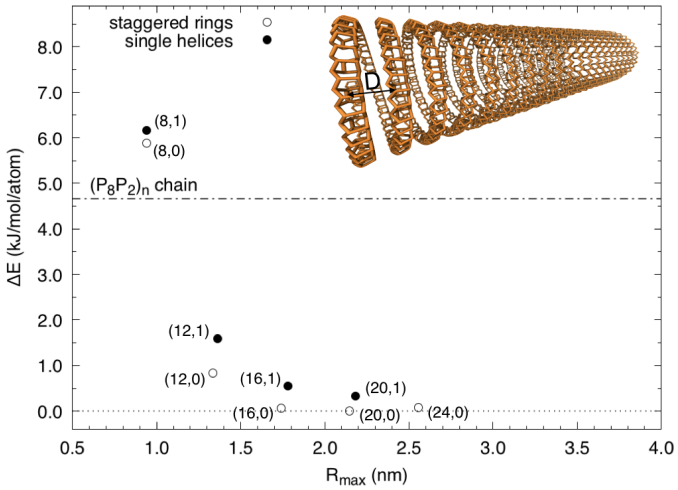

Figure 4: The relative energy of the single-chain $(n_1,1)$ helices and the staggered stacked $(P_8P_2)_n$ rings as a function of the maximum radius. The top inset shows the structure of (20,1) helix.

The relative energies of single-chain helices and staggered stacked rings are compared in Figure 4. It turns out that the staggered stacked rings are more stable in comparison to the single-chain helices for all studied rolling vectors. However, the difference is only 0.3 kJ/mol per atom for (20,1) and (20,0). Consequently, the (20,1) helix is 8.6 kJ/mol per atom less stable than black phosphorus at the same level of theory. It was not computationally feasible to calculate the next largest (24,1) single-chain helix at the PBE0-D3/TZVPP level of theory (5770 atoms in the unit cell), but using a smaller split-valence-polarized (SVP) basis set we found out that the relative energy of the next largest (24,1) helix was only 0.02 kJ/mol per atom lower than for (20,1). We thus expect

the energy minimum of the single-chain helices in this region of n_1 values.

The single-chain (n_1,1) helices are similar to the "helical coil allotrope" recently discussed by Tománek *et al.*[17]. Combining structure and energy data from non-dispersion-corrected DFT-LDA and DFT-PBE calculations with an analytical model, they predicted a minimum energy diameter of 4.2 nm and inter-loop distance of 0.65 nm (4.8 nm and 0.73 nm with PBE). These values resemble the diameter and inter-loop distance in our (20,1) helix (4.73 nm and 0.65 nm, respectively). It was not possible to carry out harmonic frequency calculations on the (n_1,1) helices due to their enormous unit cell sizes.

We finish by describing the cases where $n_2 > 1$. To our knowledge, such structures have not been discussed in the literature ever. As illustrated in Figure 1c, the values $n_2 > 1$ mean that several $(P_8P_2)_n$ chains are coiled into helical shape at the same time. As an example, consider the bottom panel in Figure 2, which illustrates (20,20) structure with 20 intertwined helices. We studied such multi-chain helices for n_1 = 8, 12, 16, 20, and 24, considering several values of n_2 for each case. The full list of studied multi-chain helices is available in the Supporting Information, together with a figure of (12,n_2) helices. The relative energies of all studied $(P_8P_2)_n$ helices are plotted in Figure 5 as a function of the chiral angle, θ, which connects the n_1 and n_2 vectorsand reveals smooth trends in the data series.

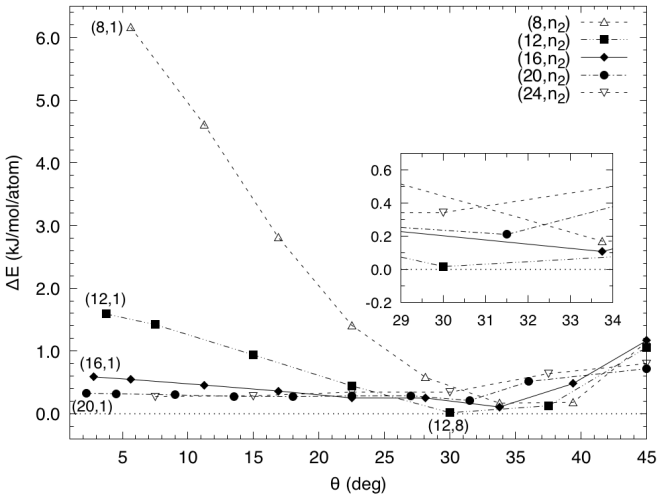

Figure 5: The relative energy of all studied $(P_8P_2)_n$ helices as a function of the chiral angle θ (see Figure 1c). The energies are given relative to the structure (20,0), that is, staggered stacked P_{200} rings). The inset shows a magnification on the minimum energy region. The single-chain (n_1,1) helices and the (12,8) multi-chain helix are labeled for clarity. The other data points are multi-chain helices (see text).

Looking at Figure 5, it is clear that (8,n_2) series shows the largest variation as a function of the θ angle. For the (12,n_2) series, the energy already varies much less and this series also shows the helical structure with the lowest absolute energy. The (12,8) structure is practically isoenergetic with the (20,0) stacked staggered rings, being only 0.02 kJ/mol per atom less stable. Up until the (20,n_2) helices, the minimum energy structure of each n_1 series is located within θ = 30–34°.

The multi-chain helices possess a special case $n_1 = n_2$, where harmonic frequency calculations are feasible due to smaller unit cell size. We were able to confirm the (12,12) helix with 240 atoms in the unit cell as a true local minimum. In other words, coiling the $(P_8P_2)_n$ chain into a helical shape appears to result in true local minima. The true local minimum character is encouraging from the point of view of experimental realization within a suitable templating approach. Considering the experimental feasibility of the various helix structures, the synthesis of single-chain (n_1,1) helices seems conceptually simpler than the self-assembly of a multi-chain helix structure with $n_2 > 1$. The formation of multi-chain helices would be a two-stage process: First, the formation of several single-chain helices would be required and secondly, the single-chain helices would then need to self-assemble into an intertwined structure.

Concerning the electronic properties of all studied structures, they turned out to be wide-band gap semiconductors at the chosen level of theory. For most structures, the predicted fundamental electronic band gap lies at the border of visible/UV regions, in the range of 3.0-3.4 eV (see SI). As a future study, it will be of interest to investigate optical band gaps via suitable TD-DFT approaches.

The spring-like appearance of the single-chain (n_1,1) helices raises the question of their elastic properties. We calculated the Young's modulus, that is, the stiffness of the (12,1) single-chain helix (see SI for the details). Our estimate of Young's modulus is 5 GPa, which is a rather low stiffness and in the regime typically reported for polymers such as Nylon (6.6 GPa).[21]

In conclusion, we have derived the structural principles of phosphorus nanorings and nanohelices built from $(P_8P_2)_n$ chains. Such structures were first suggested over 20 years ago by Böcker and Häser.[13] Today, quantum chemical calculations on nanohelices with thousands of atoms in the unit cell are feasible when the structures are systematically built up and calculated exploiting full helical symmetry. Some of the ring-shaped materials studied here have been recently synthetized inside carbon nanotube templates and further tuning of the templating approach could result in yet undiscovered phosphorus allotropes. The predicted phosphorus nanohelices possess interesting mechanical properties and the systematic construction scheme illustrated here can also be applied to derive other inorganic helical materials with fascinating structures and properties.

Methods. The first-principles calculations were performed within the framework of Density Functional Theory (DFT), using the hybrid PBE0 exchange-correlation

functional.[22] Van der Waals dispersion interactions were taken into account using Grimme's empirical DFT-D3 method with zero-damping (ZD) and three-body ABC contributions.[23,24] All calculations were carried out with a development version of the CRYSTAL code,[25] exploiting full helical symmetry to speed up the calculations.[19] CRYSTAL expands the crystal orbitals as linear combinations of atom-centered Gaussian-type functions. We applied a triple-ζ-valence quality basis set (TZVPP) derived from the molecular Karlsruhe basis set.[26] The applied DFT-PBE0-D3(ZD+ABC)/TZVPP level of theory produces very reasonable geometries for known phosphorus allotropes. Benchmark calculations and full computational details are discussed in the Supporting Information.

Acknowledgments. Computational resources were provided by CSC, the Finnish IT Center for Science. G. S. gratefully acknowledges financial support from the Erasmus+ Traineeship.

Keywords: Phosphorus, Allotropy, Helical structures, Nanostructures, Density functional calculations

* Electronic address: antti.j.karttunen@iki.fi

[1] F. Bachhuber, J. von Appen, R. Dronskowski, P. Schmidt, T. Nilges, A. Pfitzner, and R. Weihrich, Angew. Chem. Int. Ed. **53**, 11629 (2014).
[2] M. Schöneich, A. Hohmann, P. Schmidt, F. Pielnhofer, F. Bachhuber, R. Weihrich, O. Osters, M. Köpf, and T. Nilges, Z. Kristallogr. **232**, 91 (2017).
[3] V. Sorkin, Y. Cai, Z. Ong, G. Zhang, and Y. W. Zhang, Crit. Rev. Solid State **42**, 1 (2017).
[4] R. Gusmão, Z. Sofer, and M. Pumera, Angew. Chem. Int. Ed. **56**, 8052 (2017).
[5] F. Bachhuber, J. von Appen, R. Dronskowski, P. Schmidt, T. Nilges, A. Pfitzner, and R. Weihrich, Z. Kristallogr. **230**, 107 (2015).
[6] M. Ruck, D. Hoppe, B. Wahl, P. Simon, Y. Wang, and G. Seifert, Angew. Chem. Int. Ed. **44**, 7616 (2005).
[7] N. Eckstein, A. Hohmann, R. Weihrich, T. Nilges, and P. Schmidt, Z. Anorg. Allg. Chem. **639**, 2741 (2013).
[8] H. Thurn and H. Krebs, Acta Crystallogr. B **25**, 125 (1969).
[9] A. Pfitzner, M. F. Bräu, J. Zweck, G. Brunklaus, and H. Eckert, Angew. Chem. Int. Ed. **43**, 4228 (2004).
[10] R. Jones and D. Hohl, J. Chem. Phys. **92**, 6710 (1990).
[11] R. Jones and G. Seifert, J. Chem. Phys. **96**, 7564 (1992).
[12] G. Seifert and R. Jones, Z. Phys. D **26**, 349 (1993).
[13] S. Böcker and M. Häser, Z. Anorg. Allg. Chem. **621**, 258 (1995).
[14] A. J. Karttunen, M. Linnolahti, and T. A. Pakkanen, Chem.–Eur. J. **13**, 5232 (2007).
[15] P. Nava and R. Ahlrichs, Chem. – Eur. J. **14**, 4039 (2008).
[16] J. Zhang, D. Zhao, D. Xiao, C. Ma, H. Du, X. Li, L. Zhang, J. Huang, H. Huang, C.-L. Jia, et al., Angew. Chem. Int. Ed. **56**, 1850–1854 (2017).
[17] D. Liu, J. Guan, J. Jiang, and D. Tománek, Nano Lett. **16**, 7865 (2016).
[18] D. Pfister, K. Schäfer, C. Ott, B. Gerke, R. Pöttgen, O. Janka, M. Baumgartner, A. Efimova, A. Hohmann, P. Schmidt, et al., Adv. Mater. **28**, 9783 (2016).
[19] Y. Noël, P. D'arco, R. Demichelis, C. M. Zicovich-Wilson, and R. Dovesi, J. Comput. Chem. **31**, 855 (2010).
[20] C. T. White, D. H. Robertson, and J. W. Mintmire, Phys. Rev. B **47**, 5485 (1993).
[21] B. Ellis and R. Smith, *Polymers: a property database* (CRC Press, 2008), 2nd ed.
[22] C. Adamo and V. Barone, J. Chem. Phys. **110**, 6158 (1999).
[23] S. Grimme, J. Antony, S. Ehrlich, and H. Krieg, J. Chem. Phys. **132**, 154104 (2010).
[24] T. Risthaus and S. Grimme, J. Chem. Theory Comput. **9**, 1580 (2013).
[25] R. Dovesi, R. Orlando, A. Erba, C. M. Zicovich-Wilson, B. Civalleri, S. Casassa, L. Maschio, M. Ferrabone, M. D. L. Pierre, P. D'Arco, et al., Int. J. Quant. Chem. **114**, 1287 (2014).
[26] F. Weigend and R. Ahlrichs, Phys. Chem. Chem. Phys. **7**, 3297 (2005).
[27] M. Hart, E. R. White, J. Chen, C. M. McGilvery, C. J. Pickard, A. Michaelides, A. Sella, M. S. P. Shaffer, and C. G. Salzmann, Angew. Chem. Int. Ed. **56**, 8144 (2017).
[28] On p. 279 of ref.[13], Böcker and Häser note that "... pure chains of]P2[P8] bend on themselves and can only form huge macrocycles or corresponding large-diameter helices, that is, low density aggregates".
[29] We note that in another recent study white phosphorus has been encapsulated and polymerized inside single-walled CNTs with an average diameter of 8.1 Å.[27]
[30] Only structures with $n_1 \geq n_2$ were investigated, corresponding to restricting the rolling vector to the irreducible wedge.[20] For the phosphorus helices, the maximum θ, that contains all possible symmetry-nonequivalent rolling directions, is 45°. In the case of graphene and CNT, the primitive cell is hexagonal with a maximum θ of 30°.
[31] The diameter reported for P_{240} includes two times the van der Waals radius of phosphorus

Table of contents entry

Phosphorus nanohelices: We present the family tree of curved red phosphorus modifications and introduce novel phosphorus nanohelices with exciting mechanical properties.